Remote Substituent Effects on the Oxymercuration of 2-Substituted Norbornenes: An Experimental and Theoretical Study

Peter Mayo, Galina Orlova, John D. Goddard,*,† and William Tam*,‡

Guelph-Waterloo Centre for Graduate Work in Chemistry and Biochemistry, Department of Chemistry and Biochemistry, University of Guelph, Guelph, Ontario, Canada N1G 2W1

wtam@uoguelph.ca

Received March 28, 2001

The effect of a remote substituent on regioselectivity in the oxymercuration of 2-substituted norbornenes has been investigated experimentally and theoretically using density functional theory (DFT). Regioselectivities of 1:1 to 14:1 were observed with various 2-substituted norbornenes. Exo-2-substituted norbornenes always gave greater regioselectivities compared to the corresponding endo-2-substituted norbornenes. The effects of solvents on the regioselectivity have also been examined, and ethereal solvents were found to be the best choice giving the optimal yield and regioselectivity. The relative rate of oxymercuration was estimated by competition experiments. The least reactive substrate (X = OAc) gave the highest regioselectivity. According to DFT predictions, the increased difference between the reaction barriers that results in the greater regioselectivity is correlated directly with the larger polarity of the C=C double bond, which is attacked by the mercury and oxygen. A number of stable exo and endo conformers were predicted. All exo conformers show the same polarity of the double bond, while some endo conformers have a reversal of this polarity. All the conformers except those with the OAc substituent are very close in energy and thus should react. The existence of a mixture of endo conformers with the C=C double bond of opposite polarity clearly explains a decrease in regioselectivity for the endo species. The origin of the greatest regioselectivity for the OAc-2-norbornenes lies in the fact that the conformer with the largest polarity is notably lower in energy than others due to an internal C−H−O hydrogen bond.

Introduction

The study of the long-range stereoelectronic effects of a remote substituent in controlling the regio- and stereoselectivities in nucleophilic and electrophilic additions to π-bonds has attracted considerable interest.[1,2] To date, studies of such an effect on the bicyclo[2.2.1]heptane and bicyclo[2.2.2]octane systems (Figure 1) include the following: nucleophilic additions of hydride and alkyllithium reagents to 7-norbornanones **1** and bicyclo[2.2.2]-octan-2-ones **2**;[3] Baeyer−Villiger oxidation with peracids and ring expansion with diazomethane of **1**;[4,5] electrophilic additions of dichlorocarbene to 7-methylenenorbornenes **3**;[6] hydroboration, epoxidation, and oxymercuration of **3**;[7] electrophilic additions of PhSeX (X = Cl, Br), PhSCl, and Br_2 to 7-oxabicyclo[2.2.1]hept-5-ene derivatives **4**;[8,9] 1,3-dipolar cycloadditions; Diels−Alder cycloadditions and Pauson-Khand reactions of **4**;[10−12] ring-

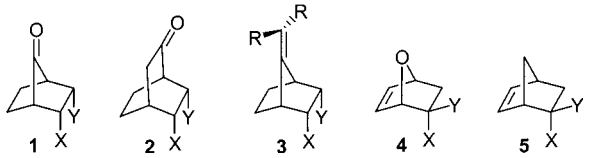

Figure 1. Bicyclo[2.2.1]heptane and bicyclo[2.2.2]octane systems.

* To whom correspondence should be addressed. Tel: 519-824-4120.
† Fax: 519-766-1499. E-mail: (J.D.G.) jgoddard@uoguelph.ca.
‡ E-mail: wtam@uoguelph.ca.

(1) (a) Cieplak, A. S.; Tait, B. D.; Johnson, C. R. *J. Am. Chem. Soc.* **1989**, *111*, 4635. (b) Adcock, W.; Cotton, J.; Trout, N. A. *J. Org. Chem.* **1994**, *59*, 1867. (c) Gung, B. W. *Tetrahedron* **1996**, *52*, 5263. (d) Fraser, R. R.; Faibish, N. C.; Kong, F.; Bednarski, J. *J. Org. Chem.* **1997**, *62*, 6167.

(2) For recent reviews, see: (a) Cieplak, A. S. *Chem. Rev.* **1999**, *99*, 1265. (b) Ohwada, T. *Chem. Rev.* **1999**, *99*, 1337. (c) Mehta, G.; Chandrasekhar, J. *Chem. Rev.* **1999**, *99*, 1437.

(3) (a) Mehta, G.; Khan, F. A. *J. Am. Chem. Soc.* **1990**, *112*, 6140. (b) Mehta, G.; Khan, F. A.; Ganguly, B.; Chandrasekhar, J. *J. Chem. Soc., Chem. Commun.* **1992**, 1711. (c) Ganguly, B.; Chandrasekhar, J.; Khan, F. A.; Mehta, G. *J. Org. Chem.* **1993**, *58*, 1734. (d) Mehta, G.; Khan, F. A.; Ganguly, B.; Chandrasekhar, J. *J. Chem. Soc., Perkin Trans. 2* **1994**, 2275. (e) Mehta, G.; Khan, F. A.; Adcock, W. *J. Chem. Soc., Perkin Trans. 2* **1995**, 2189. (f) Mehta, G.; Khan, F. A.; Mohal, N.; Narayan, I. N.; Kalyanaraman, P.; Chandrasekhar, J. *J. Chem. Soc., Perkin Trans. 1* **1996**, 2665. (g) Mehta, G.; Ravikrishna, C.; Kalyanaraman, P.; Chandrasekhar, J. *J. Chem. Soc., Perkin Trans. 1* **1998**, 1895.

(4) Mehta, G.; Mohal, N. *J. Chem. Soc., Perkin Trans. 1* **1998**, 505.
(5) Mehta, G.; Khan, F. A. *J. Chem. Soc., Perkin Trans. 1* **1993**, 1727.
(6) Mehta, G.; Gunasekaran, G. *J. Org. Chem.* **1994**, *59*, 1953.
(7) (a) Mehta, G.; Khan, F. A. *J. Chem. Soc., Chem. Commun.* **1991**, 18. (b) Mehta, G.; Khan, F. A.; Gadre, S. R.; Shirsat, R. N.; Ganguly, B.; Chandrasekhar, J. *Angew. Chem., Int. Ed. Engl.* **1994**, *33*, 1390.
(8) (a) Arjona, O.; de la Pradilla, R. F.; Plumet, J.; Viso, A. *Tetrahedron* **1989**, *45*, 4565. (b) Arjona, O.; de la Pradilla, R. F.; Pita-Romero, I.; Plumet, J.; Viso, A. *Tetrahedron* **1990**, *46*, 8199.
(9) Arjona, O.; de la Pradilla, R. F.; Garcia, L. Mallo, A.; Plumet, J. *J. Chem. Soc., Perkin Trans. 2* **1989**, 1315.
(10) Arjona, O.; Manzano, C.; Plumet, J. *Heterocycles* **1993**, *35*, 63 and refererences cited therein.
(11) Black, K. A.; Vogel, P. *J. Org. Chem.* **1986**, *51*, 5341.
(12) Arjona, O.; Csákÿ, A. G.; Murcia, M. C.; Plumet, J. *J. Org. Chem.* **1999**, *64*, 7338.

10.1021/jo010330h CCC: $20.00
Published on Web 07/04/2001

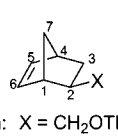

6a: X = CH_2OTBS
6b: X = COOMe
6c: X = OH
6d: X = OBn
6e: X = OTBS
6f: X = OCOPh
6g: X = OCO-C_6H_4-*p*-NO_2
6h: X = OAc

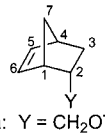

7a: Y = CH_2OTBS
7b: Y = COOMe
7c: Y = OH
7d: Y = OBn
7e: Y = OTBS
7f: Y = OAc

Figure 2. Exo- and endo-2-substituted norbornenes.

Scheme 1

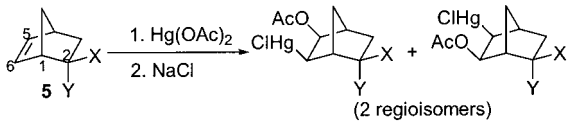

Scheme 2

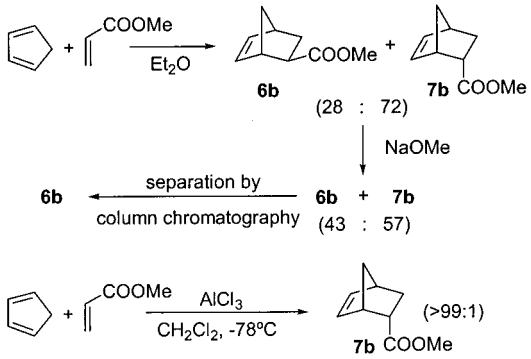

opening cross-coupling metathesis of **4**;[13] and hydroboration and electrophilic addition of PhSeX (X = Cl, Br) and PhSCl to 2-substituted norbornenes **5**.[14,15] In this paper, we report our experimental and theoretical results on remote substituent effects on regioselectivity in the oxymercuration of 2-substituted norbornenes **5** (Scheme 1).[16]

Results and Discussion

Synthesis of 2-Substituted Norbornenes. To study substituent effects on regioselectivity in the oxymercuration of 2-substituted norbornenes, exo-2-substituted norbornenes **6a**−**h** and endo-2-substituted norbornenes **7a**−**f** were prepared (Figure 2). The *exo*-and *endo*-norbornenes **6b** and **7b** were prepared by Diels−Alder reactions (Scheme 2). A thermal Diels−Alder reaction of cyclopentadiene and methyl acrylate, followed by epimerization of the endo/exo cycloadduct mixture with NaOMe and separation of the exo and endo cycloadducts by column chromatography, produced *exo*-norbornene **6b**.[17a]

Scheme 3

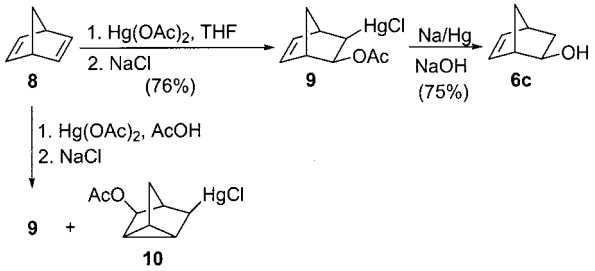

Scheme 4

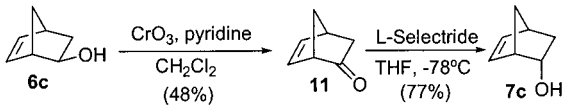

The *endo*-norbornene **7b** was prepared from the Lewis acid-catalyzed Diels−Alder reaction of cyclopentadiene and methyl acrylate.[17b,c] Reduction of **6b** and **7b** by $LiAlH_4$ followed by protection with TBSCl provided the *exo*-norbornene **6a** and the *endo*-norbornene **7a**. The *exo*-norbornene **6c** was prepared from norbornadiene **8** (Scheme 3). According to the literature, the oxymercurial compound **9** could be made by oxymercuration using $Hg(OAc)_2$ in AcOH.[18] However, we found that under these reaction conditions a significant amount of a rearrangement product, the tricyclic compound **10**, was formed accompanied by the desired oxymercurial compound **9**, and separation of these compounds by chromatography was very difficult. After several attempts to modify the reaction conditions, we found that using THF as solvent and slow addition of $Hg(OAc)_2$ to an excess of norbornadiene **8** led to the exclusive formation of the desired oxymercurial compound **9**. Demercuration and hydrolytic cleavage of the acetate group was achieved in a single step using sodium amalgam in NaOH to afford the required *exo*-norbornene **6c** in good yield. Oxidation of **6c** followed by reduction with L-Selectride at −78 °C provided the endo alcohol **7c** with >99:1 endo/exo selectivity (Scheme 4). Derivatization of **6c** and **7c** gave the *exo*-norbornenes **6d**−**h** and *endo*-norbornenes **7d**−**f**.

Oxymercuration of 2-Substituted Norbornenes. Unlike the oxymercuration of monocyclic olefin systems that usually follows anti addition, oxymercuration of bicyclic olefins often gives syn addition products. Traylor and Baker have shown that oxymercuration of norbornene (X = H) gave entirely the syn-exo product.[19] In accord with this result, oxymercuration of all the 2-substituted norbornenes in our study was highly stereoselective, giving only the syn-exo products. Two different regioisomers can be formed in the syn oxymercuration of 2-exo-substituted norbornenes (Table 1). Hg could end up on C_6 (giving regioisomer **12**) or on C_5 (giving regioisomer **13**). Addition of 1.2−3 equiv of $Hg(OAc)_2$ to 2-substituted norbornenes **6a**−**h** in THF afforded a mixture of regioisomers in moderate to good yields. Oxymercuration of **6a** with an essentially neutral substituent (X = CH_2OTBS) was not selective, giving a 1:1

(13) Arjona, O.; Csákÿ, A. G.; Murcia, M. C.; Plumet, J. *J. Org. Chem.* **1999**, *64*, 9739.
(14) Brands, K. M. J.; Kende, A. S. *Tetrahedron Lett.* **1992**, *33*, 5887.
(15) Arjona, O.; de la Pradilla, R. F.; Plumet, J.; Viso, A. *J. Org. Chem.* **1991**, *59*, 6227.
(16) For preliminary results of this work, see: Mayo, P.; Poirier, M.; Rainey, J.; Tam, W. *Tetrahedron Lett.* **1999**, *40*, 7727.
(17) (a) Cope, A. C.; Ciganek, E.; Lebel, N. A. *J. Am. Chem. Soc.* **1959**, *81*, 2799. (b) Inukai, T.; Kojima, T. *J. Org. Chem.* **1966**, *31*, 2032. (c) Sauer, J.; Kredel, J. *Tetrahedron Lett.* **1966**, 713.
(18) Bartsch, R. A.; Lee, J. G. *J. Org. Chem.* **1991**, *56*, 2579.
(19) (a) Traylor, T.; Baker, A. *Tetrahedron Lett.* **1959**, 14. (b) Traylor, T.; Baker, A. *J. Am. Chem. Soc.* **1963**, *85*, 2746. (c) Traylor, T. *J. Am. Chem. Soc.* **1964**, *86*, 244. (d) Whitesides, G. M. Fillpo, J. S. *J. Am. Chem. Soc.* **1970**, *92*, 6611. (e) Jensen, F. R.; Miller, J. J.; Cristol, S. J.; Beckley, R. S. *J. Org. Chem.* **1972**, *37*, 4341.

Table 1. Oxymercuration of *Exo*-2-substituted Norbornenes

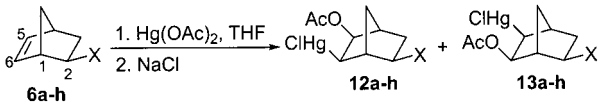

entry	norbornene	X	yield[a] (%)	**12**:**13**[b]
1	**6a**	CH_2OTBS	91	1:1
2	**6b**	COOMe	72	5:1
3	**6c**	OH	49	6:1
4	**6d**	OBn	58	9:1
5	**6e**	OTBS	83	12:1
6	**6f**	OCOPh	83	12:1
7	**6g**	$OCO-C_6H_4$-*p*-NO_2	74	14:1
8	**6h**	OAc	75	14:1

[a] Isolated yields of pure products after chromatography. [b] Measured by intergration of 400 MHz ^{1}H NMR spectra before and after column chromatography.

Table 2. Oxymercuration of Endo-2-Substituted Norbornenes

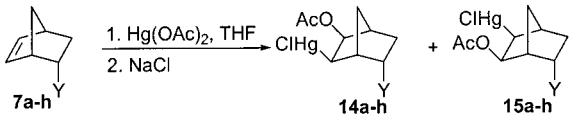

entry	norbornene	X	yield[a] (%)	**14**:**15**[b]
1	**7a**	CH_2OTBS	80	1:1
2	**7b**	COOMe	62	5:1
3	**7c**	OH	30	3:1
4	**7d**	OBn	36	6:1
5	**7e**	OTBS	69	4:1
6	**7f**	OAc	49	9:1

[a] Isolated yields of pure products after chromatography. [b] Measured by intergration of 400 MHz ^{1}H NMR spectra before and after column chromatography.

mixture of regioisomers **12a** and **13a**. With an ester (COOMe) functionality, **6b** gave a moderate regioselectivity of 5:1. With oxy substituents, the regioselectivities increased further. When X was changed from OH to OBn, to OTBS, and to OCOR, the regioselectivities increased from 6:1 to 14:1. The highest regioselectivity was obtained with X= OAc. The oxymercuration reaction of 2-endo-substituted norbornenes **7a**−**f** is shown in Table 2. Although a similar trend was observed, the regioselectivities of the endo substituents ranged from 3:1 to 9:1, and these were consistently lower than the corresponding ratios for the exo substituents.

Several competition experiments were carried out in order to estimate the relative rates of oxymercuration of 2-substituted norbornenes. For example, a mixture of equimolar amounts of **6c** and **6h** was allowed to react with 0.25 equiv of $Hg(OAc)_2$ (in order to approach pseudo-first-order conditions), and the relative rate of oxymercuration of **6c** and **6h** was determined by the ratio of the oxymercuration products, which was measured from the integration of the 400 MHz ^{1}H NMR spectrum of the crude reaction mixture. Similar competition experiments were carried out between various norbornenes and **6c**, and the results are shown in Table 3. The rates of oxymercuration of all the norbornenes examined (with $X \neq H$) are slower than norbornene (X = H). Although there is no good correlation between the relative rate of oxymercuration and the regioselectivity observed, the most reactive substituted norbornene (**6a**) gave the lowest regioselectivity and the least reactive substituted norbornene (**6h**) gave the highest regioselectivity.

Table 3. Relative Rate of Oxymercuration of *Exo*-2-substituted Norbornenes in THF

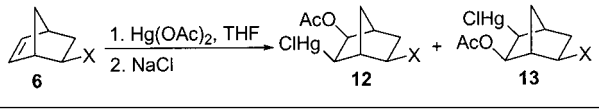

entry	norbornene	X	relative rate	**12**:**13**
1	**6i**	H	8.6	
2	**6a**	CH_2OTBS	7.8	1:1
3	**6c**	OH	4.3	6:1
4	**6e**	OTBS	2.3	12:1
5	**6d**	OBn	2.3	9:1
6	**6b**	COOMe	1.6	5:1
7	**6h**	OAc	1	14:1

Table 4. Effect of Solvent in Oxymercuration of Norbornene 6h

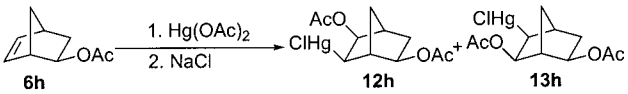

entry	solvent	yield[a] (%)	**12h**:**13h**[b]
1	toluene	91	6:1
2	DMF	68	7.5:1
3	CH_3CN	75	9:1
4	DME	91	14:1
5	Et_2O	68	14:1
6	THF	99	14:1
7	CH_2ClCH_2Cl	92	14:1
8	hexanes	84	15:1

[a] Isolated yields of pure products after chromatography. [b] Measured by intergration of 400 MHz ^{1}H NMR spectra before and after column chromatography.

The effects of different solvents used in the oxymercuration of norbornene **6h** (X = OAc) were studied, and the results are shown in Table 4. Although the use of an aromatic solvent such as toluene still provided a good yield in the oxymercuration, the regioselectivity was much lower than that obtained using THF as solvent (Table 4, entry 1). Oxymercuration in DMF and CH_3CN also gave lower regioselectivities as well as lower yields (Table 4, entries 2 and 3). The use of ethereal solvents such as DME, Et_2O, and THF and a chlorinated solvent such as 1,2-dichloroethane all provided an excellent regioselectivity of 14:1 (Table 4, entries 4−7). Using hexanes as solvent gave the highest regioselectivity of 15:1 (Table 4, entry 8), although the yield was lowered to 84%.

Except for the neutral group CH_2OTBS, which showed no selectivity, the major regioisomers formed in all cases were the ones with the Hg attached to C_6 and the OAc attached to C_5 (Tables 1 and 2). The regiochemistry of all of the isomers was identified by spectroscopic techniques and/or by chemical means. NOESY experiments showed that in the major regioisomers **12** (e.g., **12e**, when X = OTBS), positive NOE were observed between H^a and H^c but no NOE were observed between H^a and H^b (Figure 3). In contrast, no NOE was observed between H^a and H^c in the minor regioisomer **13e**, but a positive NOE was observed between H^a and H^b. We have also confirmed this identification by chemical means. For example, for the regioisomers **12e** and **13e** with X = OTBS, the regioisomers were converted to **16e** and **17e** by demercuration with Na/Hg in NaOH or with $LiAlH_4$, followed by protection with TBSCl (Scheme 5). Compound **16e** is C_2-symmetric, and therefore, only four carbon signals from the bicyclic framework were observed in the ^{13}C NMR

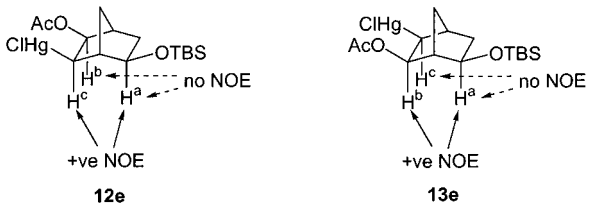

Figure 3. Determination of regiochemistry by NOE.

Scheme 5

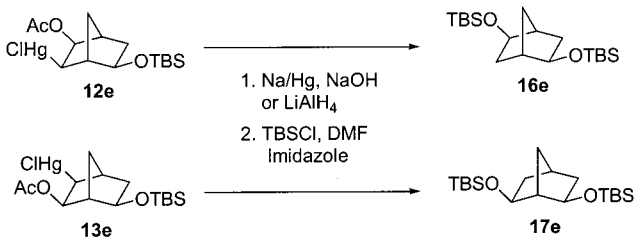

Scheme 6

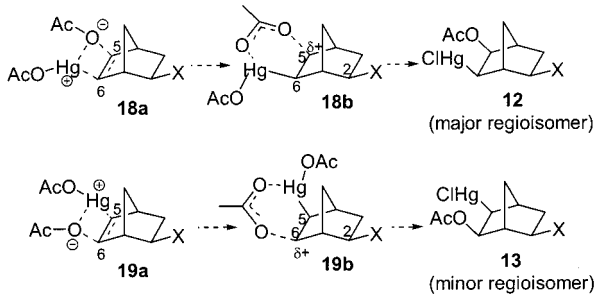

spectrum. In the case of compound **17e**, a plane of symmetry is present in the norbornane, and therefore, five carbon signals from the bicyclic framework were observed in the ^{13}C NMR spectrum.

Unlike the oxymercuration of monocyclic olefin systems which usually follows anti addition, oxymercuration of bicyclic olefins often gives syn addition products.[19] Cyclic transition states have been proposed to account for these results. Thus, for the oxymercuration of unsymmetrically substituted bicyclic alkenes, the regioselectivity of the syn addition of Hg−OAc across the double bonds will be dependent on the following: (i) the charge distribution of the olefinic carbons in the Hg-olefin complex and (ii) the relative stability of the partial cations once the Hg-carbon bond has formed. In our study, the major regioisomers (**12**) in all cases were formed with the OAc attached to C_5 and the HgOAc attached to C_6 (Scheme 6). Initial complexation of $Hg(OAc)_2$ with the double bond in the norbornenes will lead to the formation of the Hg−olefin complexes **18a** and **19a**. The charge distribution in these complexes of Hg to the double bond will be one factor that influences the regioselectivity of the oxymercuration. Attack of the mercury on C_5 (**19b**) will lead to a partial positive charge on C_6, while attack on C_6 (**18b**) will lead to a partial positive charge on C_5. The relative stability of the two transition states will be another factor that controls the regioselectivity. When X is an electron-withdrawing group, the partial positive charge on C_6 expected in the transition state **19b** would be less favorable, and therefore, a transition state like **18b** would be preferred in the oxymercuration and lead to the observed major regioisomer **12**. As the electron-withdrawing power of the substituent X increases, the partial positive charge at C_6 in **19b** would be further disfavored. Thus, the formation of **18b** and the regioisomer **12** would be more probable energetically.

Theoretical Analysis. To gain further understanding of remote substituent effects on the regioselectivities in the oxymercuration of 2-substituted norbornenes as well as the relative rate of oxymercuration of these 2-substituted norbornenes, we performed a density functional study of the oxymercuration of 2-substituted norbornenes. The mechanism of the oxymercuration is of particular interest since it previously has not been examined theoretically. Our aim was to consider the charge distribution in the reactants, as well as the energetics of initial complexation of the Hg to the norbornenes and the oxymercuration reaction path itself.

Since different solvents do not change qualitatively the substituent effects and the highest regioselectivity was obtained with nonpolar solvents, the effect of media was not included in the computational research. We have examined the relative energies of and the charge distributions in conformers of *exo*- and *endo*-2-norbornenes, with OH, OAc, $OSiH_3$, OCH_3, and CH_2OH substituents. The last three groups model the experimentally used OTBS, OBn, and CH_2OTBS substituents, respectively. The potential energy profiles for the reactions of unsubstituted norbornene, of OH-*exo*-2-norbornene, of OH-*endo*-2-norbornene, and of OAc-*exo*-2-norbornene with mercury diformate, $Hg(O_2CH)_2$, are predicted. $Hg(O_2CH)_2$ was studied theoretically instead of the experimental reactant, $Hg(OAc)_2$, to lessen the computational complexity.

All theoretical predictions were performed with the GAUSSIAN 98 suite of programs.[20] The local spin density (LSD) SVWN functional with Slater exchange (S)[21] and Vosko, Wilk, and Nusair correlation (VWN)[22] and the D95V basis set[23,24] were used to predict a variety of conformers of 2-norbornenes. The charges were obtained from a natural population analysis.[25] The hybrid B3PW91 functional with Becke's B3 exchange[26] and Perdew and Wang correlation (PW91)[27] and the LanL2DZ/D95 core potential and basis set[24,28] were used for prediction of the reaction pathways. This exchange-correlation functional and these basis sets previously have predicted very

(20) Gaussian 98: Frisch, M. J.; Trucks, G. W.; Schlegel, H. B.; Scuseria, G. E.; Robb, M. A.; Cheeseman, J. R.; Zakrzewski, V. G.; Montgomery, J. A.; Stratmann, R. E.; Burant, J. C.; Dapprich, S.; Millam, J. M.; Daniels, A. D.; Kudin, K. N.; Strain, M. C.; Farkas, O.; Tomasi, J.; Barone, V.; Cossi, M.; Cammi, R.; Mennucci, B.; Pomelli, C.; Adamo, C.; Clifford, S.; Ochterski, J.; Petersson, G. A.; Ayala, P. Y.; Cui, Q.; Morokuma, K.; Malick, D. K.; Rabuck, A. D.; Raghavachari, K.; Foresman, J. B.; Cioslowski, J.; Ortiz, J. V.; Stefanov, B. B.; Liu, G.; Liashenko, A.; Piskorz, P.; Komaromi, I.; Gomperts, R.; Martin, R. L.; Fox, D. J.; Keith, T.; Al-Laham, M. A.; Peng, C. Y.; Nanayakkara, A.; Gonzalez, C.; Challacombe, M.; Gill, P. M. W.; Johnson, B. G.; Chen, W.; Wong, M. W.; Andres, J. L.; Head-Gordon, M.; Replogle, E. S.; Pople, J. A. Gaussian, Inc., Pittsburgh, PA, 1998.

(21) Slater, J. C. In *Quantum Theory of Molecular and Solids. Vol. 4: The Self-Consistent Field for Molecular and Solid*; McGraw-Hill: New York, 1974.

(22) Vosko, S. H.; Wilk, L.; Nusair, M. *Can. J. Phys.* **1980**, *58*, 1200.

(23) Leininger, T.; Nicklass, A.; Stoll, H.; Dolg, M.; Schwerdtfeger, P. *J. Chem. Phys.* **1996**, *105*, 1052.

(24) Dunning T. H., Jr.; Hay, P. J. In *Modern Theoretical Chemistry*; Schaefer, H. F., III; Plenum: New York, 1976; Vol. 3, p 1.

(25) (a) Reed, A. E.; Weinstock, R. B.; Weinhold, F. *J. Chem. Phys.* **1985**, *83*, 735. (b) Reed, A. E.; Weinhold, F.; Curtiss, L. A.; Pochatko, D., *J. Chem. Phys.* **1986**, *84*, 5687.

(26) Becke, A. D. *J. Chem. Phys.* **1993**, *98*, 5648.

(27) Burke, K.; Perdew, J. P.; Wang, Y. In *Electronic Density Functional Theory: Recent Progress and New Directions*; Dobson, J. F., Vignale, G., Das, M. P., Eds.; Plenum: New York, 1998.

(28) Hay, P. J.; Wadt, W. R. *J. Chem. Phys.* **1985**, *82*, 299.

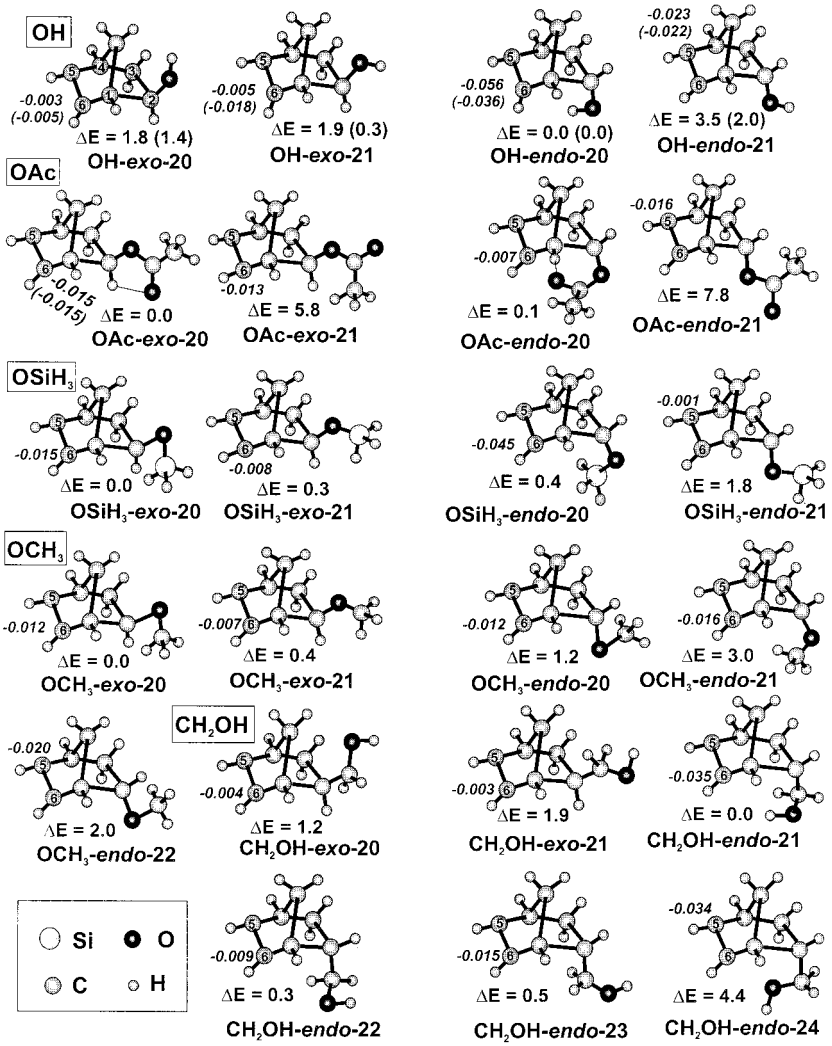

Figure 4. Conformers of *exo*- and *endo*-2-norbornenes along with the relative energies ΔE in kcal/mol predicted with the SVWN exchange-correlation functional and the D95V basis set. The positions of the excess negative charges on C_5 or C_6 determined by a natural population analysis are shown. Values in parentheses for selected 2-norbornenes were predicted with B3PW91/D95. All relative energies include zero-point vibrational energy corrections.

reasonable results for organometallic compounds.[29] The nature of each stationary point (minimum, transition state) on the adiabatic potential energy surface was verified by computation of the Hessian matrix. To confirm the connections of the saddle points to minima along the reaction pathways, Minyaev's gradient reaction line approach was used.[30] All relative energies include corrections for the zero-point vibrational energies.

Figure 4 shows the predicted conformers of the *exo*- and *endo*-2-norbornenes along with their relative energies. For OH, $OSiH_3$, OCH_3, and CH_2OH substituents, the conformers are all very close in energy (within 0.1 to 4 kcal/mol) and apparently correspond to shallow minima since the barrier to rotation about a single bond does not exceed a few kcal/mol. For the OAc-2-norbornenes, the energy differences between the conformers are somewhat greater. The lowest energy conformers, OAc-*exo*-**20** and OAc-*endo*-**20** are stabilized by weak hydrogen bonding between the hydrogen atom attached to C_2 of the norbornene and the carbonyl oxygen of the OAc substituent. Obviously, for all substituents, the predicted conformers are of relatively low energy and thus may exist at ambient temperature either in nonpolar or in weakly polar solvents.

Natural population analysis shows that the charges on the C_5 and C_6 atoms are slightly negative and slightly different. Figure 4 shows the "extra" negative charges, δ^-, located on either C_5 or C_6 of the conformers. Recall that δ^- measures the excess negative charges on one carbon center relative to the other. Naturally, the mercury atom in $Hg(O_2CH)_2$ possesses a positive charge and attack is favored on the carbon atom with the largest negative charge. We propose that the ratio "product-Hg-C_6/product-Hg-C_5" could be estimated on the basis of the relative energies of the conformers and of the position of the "extra" negative charge. The position of δ^- is predicted to depend on the remote exo and endo substituents. For the exo form, δ^- is always on C_6 for any conformation studied theoretically and with any substituent. For the endo forms, the position of δ^- depends on the conformation of the substituent and, in particular, on the orientation of the lone electron pair of the oxygen atom in the substituent. For any substituent, there exists at least one

(29) (a) Orlova G.; Scheiner, S. *J. Phys. Chem. A.* **1998**, *102*, 4813. (b) Orlova G.; Scheiner, S. *J. Phys. Chem. A.* **1998**, *102*, 260.
(30) Minyaev, R. M. *Int. J. Quantum Chem.* **1994**, *49*, 105.

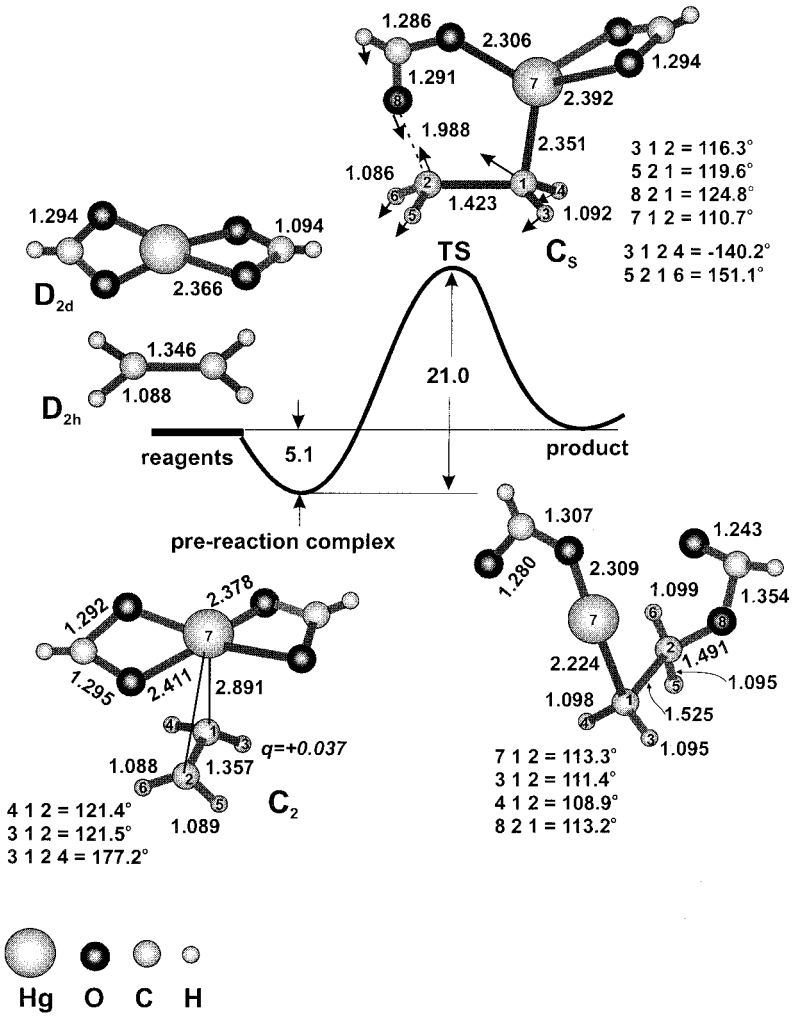

Figure 5. Potential energy profile for the reaction between $Hg(O_2CH)_2$ and ethylene predicted by B3PW91 with the LanL2DZ core potential and basis set. The relative energies (in kcal/mol) include zero-point vibrational energy corrections. The geometries are reported in angstroms and degrees. The transition-state vector is sketched. The total natural charge, *q*, on the ethylene fragment of the pre-reaction complex is reported.

conformer (with the lone pair of the oxygen oriented toward norbornene) that possesses a δ^- on C_5. Thus, for the endo forms, there is a competition between the conformers with δ^- at C_6 and the conformer or conformers with δ^- at C_5. The latter conformer is always slightly higher in energy than those with δ^- at C_6. Therefore, the endo form slightly favors the C_6 product. Such a competition is absent for the exo form, where all conformers have δ^- on C_6. Thus, the exo form shows greater regioselectivity than does the endo form.

For the exo form, the ranking of substituents (from greatest regioselectivity to least) may be established on the basis of the relative energies and the values of the "extra" negative charge at C_6: OAc > $OSiH_3$ > OCH_3 > OH ~ CH_2OH.

This order is in full accord with the experimental results. From a theoretical analysis, the OAc substituent shows the greatest regioselectivity since the OAc-*exo*-**20** and OAc-*exo*-**21** conformers possess the largest δ^- of −0.015 and −0.013, respectively. Moreover, the OAc-*exo*-**20** is 5.8 kcal/mol lower in energy than the OAc-*exo*-**21** and thus must be the predominant reactant. The $OSiH_3$ substituent is less regioselective. Although $OSiH_3$-*exo*-**20** possesses a δ^- of −0.015 similar to the OAc-*exo*-**20** case, the second conformer, $OSiH_3$-*exo*-**21**, with much smaller δ^- of −0.008, is only 0.3 kcal/mol higher in energy. Thus, $OSiH_3$-*exo*-**21** also reacts leading to less regioselectivity.

Obviously, the concept of interacting charges of the reagents is too rough an approximation to determine the whole reaction process, although it appears valid for the initial step. To examine whether the statement "the mercury prefers the carbon with the largest negative charge" remains true along the entire reaction pathway, we examined the potential energy profiles for the reaction of mercury diformate with a series of reagents. Ethylene (a simpler model reagent), unsubstituted norbornene (the parent reaction), both conformers of OH-*exo*- and of OH-*endo*-2-norbornenes, and the most stable conformer of the OAc-*exo*-2-norbornene were considered. It should be noted that the experimentally observed product ratios of 6:1 for OH-*exo*- and of 3:1 for OH-*endo*-2-norbornenes are relatively small. Such a small product ratio corresponds to a reaction involving an energy difference between the transition states of only ca. 1.0 kcal/mol. Thus, rather delicate distinctions between the reaction profiles for the various conformers should be expected.

The potential energy profile of the reaction between $Hg(O_2CH)_2$ and ethylene is shown in Figure 5. This reaction models electrophilic attack on a double bond

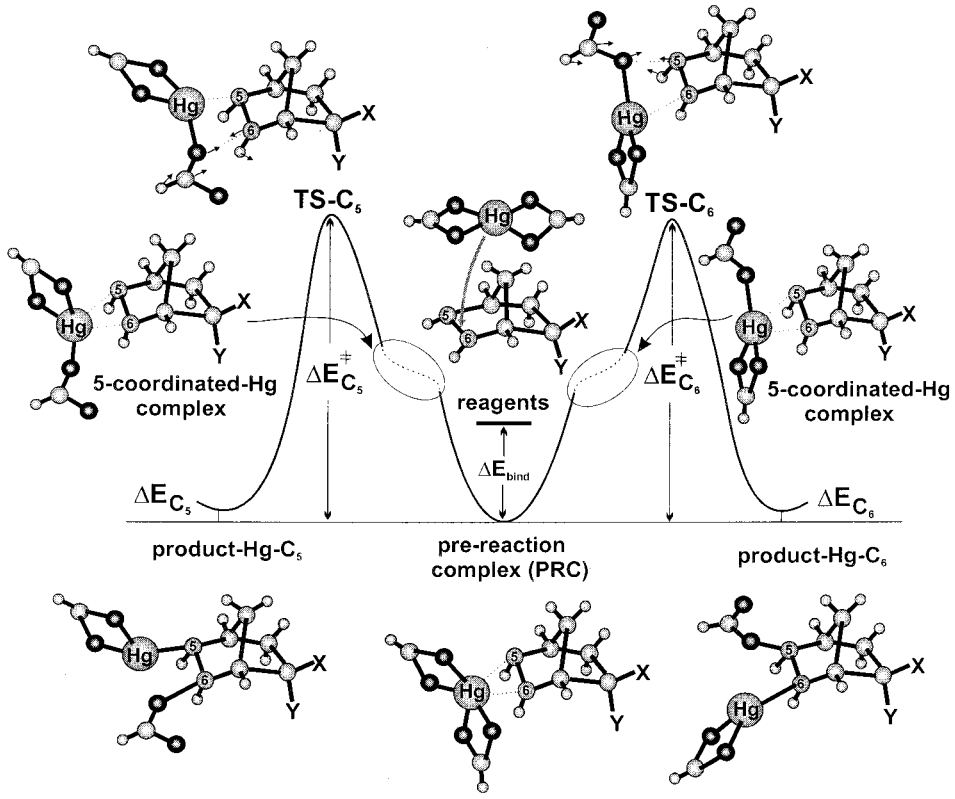

Figure 6. Potential energy profiles for the reactions between $Hg(O_2CH)_2$ and 2-substituted norbornenes (X = Y = H; X = OH, Y = H; X = H, Y = OH; X = OAc, Y = H) predicted by B3PW91 with the LanL2DZ core potential and basis set. The computed relative energies are listed in Table 5. Transition-state vectors are sketched.

without significant steric effects. $Hg(O_2CH)_2$ possesses a tetrahedral D_{2d} structure, with equal Hg−O bond lengths. The O_2CH fragments may rotate easily about the symmetry axis via a D_{2h} transition structure, with a small barrier of 1.3 kcal/mol. In the first step, a pre-reaction complex (PRC) forms, with a binding energy of 5.1 kcal/mol. The ethylene fragment possesses a slightly positive charge. A weak withdrawal of electron density from ethylene to $Hg(O_2CH)_2$ is indicative of the electrophilic character of the mercury attack on the double bond. These results are in accord with earlier theoretical predictions[31] on the reaction intermediate formed from $Hg(OAc)_2$ attack on ethylene. The PRC undergoes a rearrangement to the product via a six-membered transition structure, with a barrier of 21.0 kcal/mol. The product is essentially isoenergetic with the reactants. The transition structure possesses C_s symmetry with the bonds to be formed in the plane of the six-membered ring. The carbon which interacts with mercury is almost tetrahedral, and the C−Hg bond is only slightly longer than that in product. In contrast, the O−C interaction is at a much earlier stage, and thus, the formation of the O−C bond is the limiting step on the reaction pathway.

The potential energy profile for the reaction between $Hg(O_2CH)_2$ and the selected norbornenes is shown in Figure 6. In the first step, a PRC forms much like that in the model reaction with ethylene. Then the reaction proceeds somewhat differently. A six-membered transition structure was not located despite repeated attempts. Probably due to steric effects in the PRC, the formation of a six-membered transition structure appears to be energetically unfavorable. Instead, one of the Hg−O bonds breaks followed by a rotation of the CHO group about the remaining Hg−O bond and the reaction pathway reaches a broad plateau on the potential energy surface. This flat region is ca. 12 kcal/mol higher in energy than the PRC and corresponds to a very loose complex, with a five-coordinate mercury. Due to the extremely flat potential energy surface, we were not able to locate rigorously any critical point in this region. Since the formation of the 5-coordinated-Hg complex is a relatively low energy process, it does not appear to be the limiting step on the reaction pathway. The 5-coordinated-Hg complex transforms directly to the reaction product, product-Hg-C_5, via a four-membered transition structure, TS-C_5, or to the product-Hg-C_6 via a four-membered transition structure, TS-C_6. These transition structures, TS-C_5 and TS-C_6, are ca. 19−21 kcal/mol higher in energy than the corresponding PRC. The product-Hg-C_5 and product-Hg-C_6 are very close to or very slightly higher in energy than the PRC. Similar reaction profiles, with small deviations in the relative energies were predicted for all the norbornenes considered. Note that despite the differences in the mechanisms, the reactions of mercury diformate with ethylene, via a six-membered transition structure, and with norbornenes, via a four-membered transition structure, have similar energetics. The relative energies for the reaction profiles in Figure 6 are listed in Table 5. Selected geometrical parameters for the pre-reaction complexes, PRC, are shown in Figure 7.

For the parent reaction with norbornene, a PRC of C_s symmetry might be expected. In fact, the C_s structure is a transition state. It leads to two degenerate minima for the PRC-norbornene, upon "swinging" of the $Hg(O_2CH)_2$

(31) Yamabe, S.; Minato, T. *Bull. Chem. Soc. Jpn.* **1993**, *66*, 3339.

Table 5. Binding Energies of the PRC (ΔE_{Bind}), the Reaction Barriers for TS-C_6 ($\Delta E^{\ddagger}_{C6}$) and TS-C_5 ($\Delta E^{\ddagger}_{C5}$), the Differences between the Barriers, $\Delta\Delta E^{\ddagger}$ ($\Delta\Delta E^{\ddagger} = \Delta E^{\ddagger}_{C5} - \Delta E^{\ddagger}_{C6}$), and the Energies of the Products Referred to the PRC, ΔE_{C6} and ΔE_{C5}, for the Potential Energy Profiles in Figure 6

system	ΔE_{bind}	$\Delta E^{\ddagger}_{C6}$	$\Delta E^{\ddagger}_{C5}$	$\Delta\Delta E^{\ddagger}$	ΔE_{C6}	ΔE_{C5}
X = Y = H	−8.6	20.0	20.0	0.0	3.2	3.2
X = OH, Y = H, *exo*-**20**	−7.2	19.6	20.9	1.3	−0.3	0.9
X = OH, Y = H, *exo*-**21**	−8.0	19.4	20.2	0.8	0.0	0.6
X = H, Y = OH, *endo*-**20**	−6.3	19.9	21.5	1.6	3.1	4.8
X = H, Y = OH, *endo*-**21**	−9.0	20.0	19.2	−0.8	−0.2	1.1
X = OAc, Y = H, *exo*-**20**	−7.3	19.4	20.8	1.4	−0.4	1.1

[a] The relative energies in kcal/mol include zero-point vibrational energy corrections. All results were predicted with B3PW91/LanL2DZ.

fragment about the imaginary axis (indicated by the arrow in Figure 7), which lies in the C_s plane of the norbornene and crosses the Hg atom. The Hg−C_5 and Hg−C_6 bond lengths in PRC-norbornene are virtually equal. In contrast, for the PRC formed with all the exo forms and with OH-*endo*-**20**, the Hg−C_6 distances are notably shorter compared to Hg−C_5 while for the OH-*endo*-**21**, the Hg−C_5 bond is shorter, i.e., Hg is shifted to the carbon with the "extra" negative charge. A second possible PRC, with the Hg shifted to the carbon with the smaller negative charge does not appear to exist on the potential energy surface. For all the PRC, the total natural charges on the $Hg(O_2CH)_2$ fragments reported in Figure 7 are slightly negative. Thus, similar to the reaction with ethylene, there is a typical withdrawal of the electron density from the olefin for these electrophilic reactions. Naturally, all predicted PRC are very loose structures. Distortions of the (O_2CH) fragments involving twisting have the lowest vibrational frequencies (ca. 4−50 cm^{-1}) while those involving the stretching of the Hg−C_5 and Hg−C_6 bonds are at ca. 100 cm^{-1}. As a result, the rearrangement of the 6-coordinated PRC to the 5-coordinated Hg complex is a low energy process.

To compare the four-membered transition structure with a six-membered one, consider the geometries for the TS−C_5, TS−C_6, and corresponding products for the OH-*endo*-**20** conformer, which possesses the largest excess negative charge on C_6 among all the conformers whose reaction profiles were studied. Selected geometrical parameters are shown in Figure 8. Similar to a six-membered transition structure, the formation of the

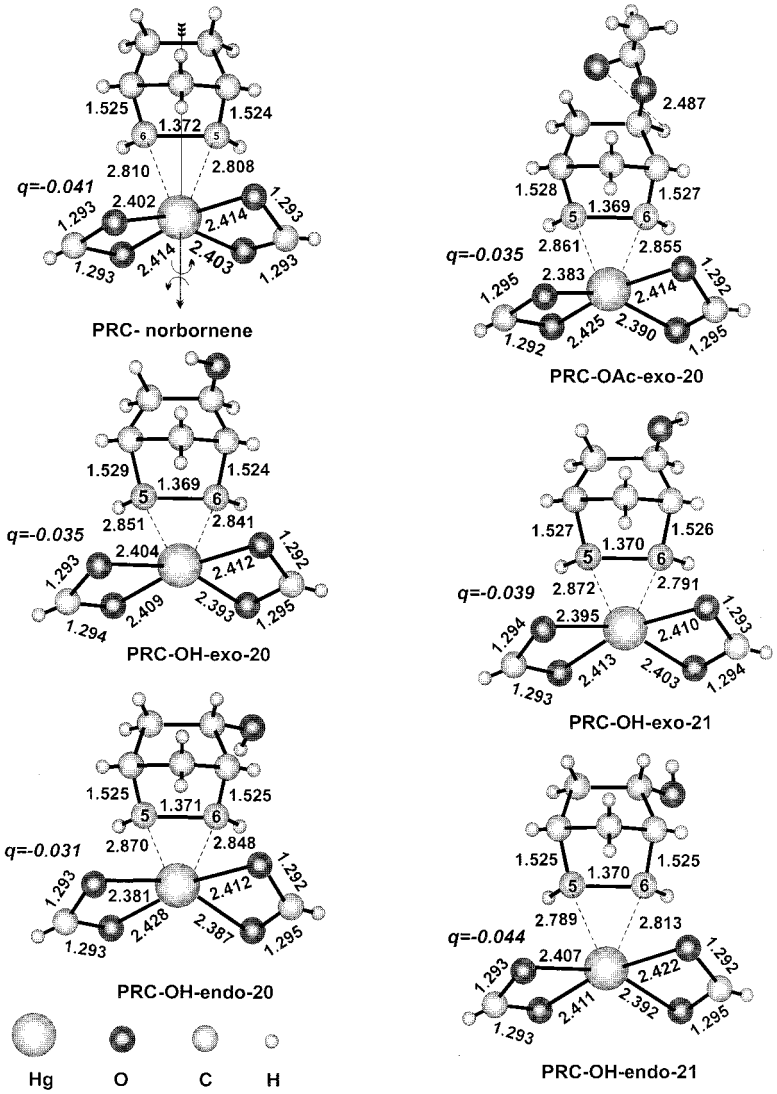

Figure 7. Selected geometrical features for the pre-reaction complexes (PRCs) of the potential energy profiles from Figure 6 as predicted using B3PW91/LanL2DZ. The geometries are reported in angstroms and degrees. The total natural charges, *q*, on the $Hg(O_2CH)_2$ fragments are reported.

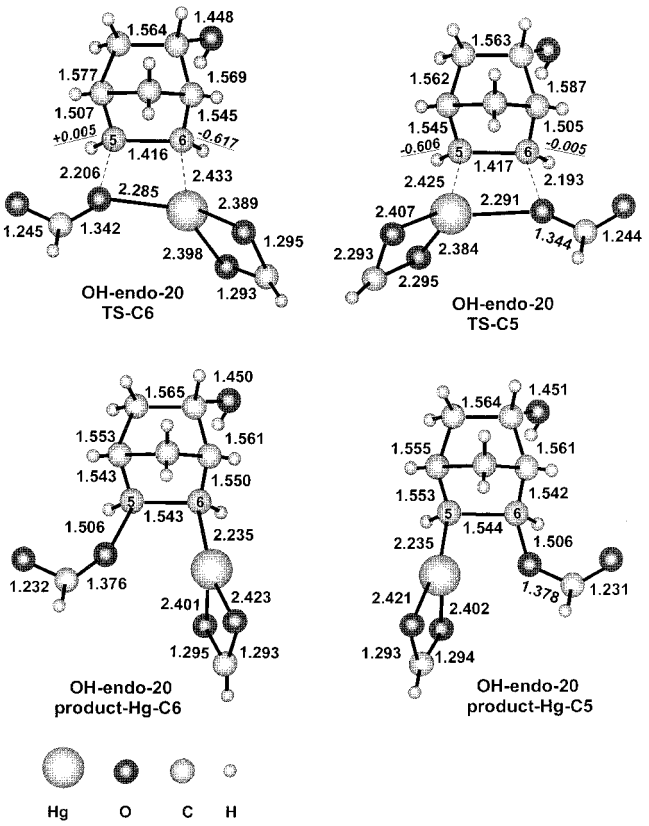

Figure 8. Selected geometrical features for the transition structures TS-C_6 and TS-C_5 and for the product-Hg-C_6 and product-Hg-C_5 of the OH-*endo*-**20** conformer as predicted using B3PW91/LanL2DZ. The geometries are reported in angstroms and degrees. Natural charges (in italics, underlined) on C_5 and C_6 are reported.

C−Hg bond is almost complete in the four-membered transition structure while the O−C interaction is at an initial stage. Thus, the formation of the O−C bond is a rate-limiting step in the oxymercuration of norbornenes similar to the reaction with ethylene. Natural charges on C_5 and C_6 in TS-C_5 and TS-C_6 in Figure 8 indicate significant withdrawal of electron density from the carbon interacting with oxygen to the carbon interacting with mercury. The TS-C_5 corresponds to a less favorable attack of mercury but, more importantly, also of oxygen since the oxygen must interact with the more negative carbon. As a result, the TS-C_5 is a later transition state than the TS-C_6.

The reaction barriers corresponding to TS-C_6 and TS-C_5 reveal the same preferences for the Hg−C and O−C interactions as do the PRC and transition structures. Table 5 shows that for OH-*exo*-**20**, OH-*exo*-**21**, OAc-*exo*-**20**, and OH-*endo*-**20**, with "extra" negative charge at C_6, the $\Delta E^{\ddagger}_{C6}$ reaction barriers are lower than $\Delta E^{\ddagger}_{C5}$ by 1.3, 0.8, 1.4, and 1.6 kcal/mol, respectively. In contrast, for OH-*endo*-**21**, which possesses the "extra" negative charge at C_5, the $\Delta E^{\ddagger}_{C5}$ is 0.8 kcal/mol lower in energy than $\Delta E^{\ddagger}_{C6}$. Thus, the presence of OH-*endo*-2 cancels the large regioselective effect of the OH-*endo*-**20**, which would be expected given the largest difference between the activation barriers. The energy difference between OH-*exo*-**20** and OH-*exo*-**21** conformers of 0.1 (1.1) kcal/mol (Figure 4) is insignificant, and both conformers are involved in the reaction. Thus, the effective $\Delta\Delta E^{\ddagger}$ ($\Delta E^{\ddagger}_{C5} - \Delta E^{\ddagger}_{C6}$) lies approximately in the middle of the range of 1.3−0.8 kcal/mol, and the resulting effect on regioselectivity becomes small. Given that the OAc-*exo*-**20**-conformer is notably more stable (5.8 kcal/mol) than the second possible conformer, OAc-*exo*-**21**, the effective $\Delta\Delta E^{\ddagger}$ should be close to 1.4 kcal/mol.

Conclusions

We have demonstrated a remarkable remote substituent effect on the regioselectivity of the oxymercuration of a 2-substituted norbornene system. Regioselectivities of 1:1−14:1 were observed with various 2-substituted norbornenes. Exo-2-substituted norbornenes always gave better regioselectivities than the corresponding *endo*-2-norbornenes. The use of ethereal solvents was found to give the highest regioselectivities in the oxymercuration reactions. Study of the relative rate of oxymercuration with various substituted norbornenes showed that the least reactive substrate (X = OAc) gave the highest regioselectivity.

Our theoretical investigations allow us to rationalize the effects of the remote substituents on regioselectivity in terms of the position of the "extra" negative charge at the carbon atoms, C_5 or C_6, which will be attacked by Hg. The positive Hg atom prefers interaction with that carbon that possesses the "extra" negative charge. The charge redistribution between C_5 and C_6 upon substitution at the 2-position of norbornene, depends on the position of the substituent (exo or endo) and on its conformation. For the exo forms, the "extra" negative charge is at C_6 for all conformers while for the endo forms there exists at least one conformer with "extra" negative charge at C_5. The competition between endo conformers with different positions of the "extra" negative charge decreases the regioselectivity compared to the exo form.

The oxymercuration of norbornenes proceeds via formation of a pre-reaction complex with a six-coordinate Hg in the initial step. This pre-reaction complex rearranges easily to a very loose complex with a five-coordinate Hg that transforms to the product via a four-membered transition structure. The preference for Hg to attack the more negative carbon remains along the whole reaction profile and results in a lowering of the activation barrier to the product of 0.8−1.6 kcal/mol compared to the "unfavorable" attack at the carbon with the smaller negative charge.

For the exo forms, the OAc-*exo*-**20** conformer with the largest "extra" negative charge is stabilized by an internal C−H···O hydrogen bond and thus is notably lower in energy than OAc-*exo*-**21**, with a smaller "extra" negative charge at C_6. Therefore, OAc-*exo*-**20** exhibits the greatest difference between the activation barriers and provides the highest regioselectivity.

Further investigations of remote substituents effects in the 2-substituted norbornene systems for other reactions are ongoing in our laboratory.

Acknowledgment. We thank the Natural Sciences and Engineering Research Council (NSERC) of Canada and the University of Guelph for generous financial support of our program. W.T. thanks Boehringer Ingelheim (Canada) Ltd. for a Young Investigator Award, and P.M. thanks NSERC for postgraduate scholarships (PGS A and PGS B). Mr. Marc Poirier and Mr. Jan Rainey are thanked for preliminary experiments, and Ms. S. N. Sullivan is thanked for preliminary analysis

of the performance of theoretical methods for the description of oxymercuration reactions. Ms. Valerie Robertson is thanked for NMR experiments and discussion of NMR data.

Supporting Information Available: Experimental procedures for preparation of substituted norbornenes and their oxymercuration reactions; Cartesian coordinates and total energies predicted theoretically for the structures in Figures 4−8; and ^{1}H and ^{13}C NMR spectra of **6a**,**e**−**g**, **7a**,**e**, **12f/13f**, and **12g/13g**. This material is available free of charge via the Internet at http://pubs.acs.org.

JO010330H